Published in final edited form as:

Cancer Prev Res (Phila). 2014 November ; 7(11): 1149–1159. doi:10.1158/1940-6207.CAPR-14-0091.

Honokiol Inhibits Lung Tumorigenesis through Inhibition of Mitochondrial Function

Jing Pan[1], **Qi Zhang**[1], **Qian Liu**[1], **Steven M. Komas**[2], **Balaraman Kalyanaraman**[2], **Ronald A. Lubet**[3], **Yian Wang**[1], and **Ming You**[1]

[1]Medical College of Wisconsin Cancer Center and Department of Pharmacology and Toxicology, Medical College of Wisconsin, 8701 Watertown Plank Road, Milwaukee, WI, USA

[2]Department of Biophysics, Medical College of Wisconsin, 8701 Watertown Plank Road, Milwaukee, WI

[3]Chemoprevention Branch, National Cancer Institute, Bethesda, MD

Abstract

Honokiol is an important bioactive compound found in the bark of Magnolia tree. It is a non-adipogenic PPARγ agonist, and capable of inhibiting the growth of a variety of tumor types both *in vitro* and in xenograft models. However, to fully appreciate the potential chemopreventive activity of honokiol, a less artificial model system is required. To that end, this study examined the chemopreventive efficacy of honokiol in an initiation model of squamous cell lung cancer (SCC). This model system uses the carcinogen N-nitroso-trischloroethylurea (NTCU) which is applied topically, reliably triggering the development of SCC within 24–26 weeks. Administration of honokiol significantly reduced the percentage of bronchial that exhibit abnormal lung SCC histology from 24.4% bronchial in control to 11.0% bronchial in honokiol treated group (p= 0.01) while protecting normal bronchial histology (present in 20.5% of bronchial in control group and 38.5% of bronchial in honokiol treated group (p= 0.004)). P63 staining at the SCC site confirmed the lung SCCs phenotype. *In vitro* studies revealed that honokiol inhibited lung SCC cells proliferation, arrested cells at the G1/S cell cycle checkpoint, while also leading to increased apoptosis. Our study showed that interfering with mitochondrial respiration is a novel mechanism by which honokiol increased generation of reactive oxygen species (ROS) in the mitochondria, triggered apoptosis, and finally leads to the inhibition of lung SCC. This novel mechanism of targeting mitochondrial suggests honokiol as a potential lung SCC chemopreventive agent.

Keywords

honokiol; N-nitroso-trischloroethylurea (NTCU); lung squamous cell carcinoma (SCC); apoptosis; mitochondria; chemoprevention

Address all correspondence to: Dr. Ming You, Medical College of Wisconsin Cancer Center and Department of Pharmacology and Toxicology, Medical College of Wisconsin, 8701 Watertown Plank Road, Milwaukee, WI 53226. myou@mcw.edu.

The authors have no conflicts of interest to disclose.

Introduction

Lung cancer is the leading cause of cancer death worldwide. Though great advances have been made in early diagnosis, discovery of chemotherapeutic agents, and in molecular oncology, many common forms of epithelial malignancy, especially carcinoma of the lung, remain difficult to cure. In this context, re-evaluation of basic assumptions about cancer is necessary. Cancer is increasingly recognized as a progressive disease, with frank malignancy representing the end stage of a chronic disease process (1). This end stage is difficult to treat compared with earlier, premalignant lesions. This raises the potential that focuses resources on the targeting of early-stage carcinogenesis may provide a way to better control cancer. This approach is defined as chemoprevention, and although a nascent field, it has experienced a number of important milestones over the past several decades that have validated this approach (2, 3). Over 80% of lung cancer is non-small cell lung carcinoma (NSCLC), with adenocarcinoma and squamous cell carcinoma (SCC) as the two major subtypes. Although research suggests that the histopathological features and molecular mechanisms of these two lung cancer subtypes are very different, treatment has generally not been tailored to specific tumor subtypes until recently.

Honokiol is an important bioactive compound present in Magnolia bark extracts, which has been used as a folk remedy for centuries in China, South Korea, and Japan to treat gastrointestinal disorders, cough, anxiety, stroke, and allergic diseases (4). Honokiol has been reported to have a variety of broad mechanisms of action, such as anti-inflammatory activity (5, 6), along with antiangiogenic (7) and cardio-beneficiating (8, 9), and neuro-protective activity (10, 11), without appreciable toxicity. Honokiol is also been identified as a naturally occurred PPARγ agonist without previously known agonist's side effect, such as adipogenesis (12). It even prevents hyperglycemia and body weight gain in diabetic mice.

In recent years, honokiol has also been demonstrated as a potential anti-tumor agent in many cancer cell lines as well as xenografts, from a variety of tumor types including glioma (13), breast cancer (14), and colorectal carcinoma (7). The combination of honokiol with other anti-cancer agents such as the mammalian target of rapamycin (mTOR) inhibitors and cisplatin had synergistic effects (15, 16). To determine the potential of honokiol as a chemopreventive agent, however, testing its efficacy in a mouse model with chemically induced precancerous lesions is necessary. In this study, we tested honokiol in the NTCU-induced mouse lung SCC model, which has been shown to be a successful mouse lung SCC model and faithfully captures well-defined, typical pathologic development from normal to bronchiolar hyperplasia, metaplasia, SCC *in situ*, and finally SCC as seen in humans(17–19).

Previous studies have shown that honokiol induces apoptosis in a variety of cancer cell lines, including murine endothelial SVR cells (6), human leukemia MOLT 4B cells (7), human colorectal carcinoma RKO cells (8) and human lung SCC CH27 cells (9). However, the precise molecular mechanism underlying the induction of apoptosis of cancer cells by honokiol still needs further investigation. Mitochondria are essential cellular organelles that play central roles in energy metabolism and apoptosis (20). During oxidative phosphorylation, electrons that escape from the mitochondrial electron transport chain react with oxygen to form $O_2^{\bullet}$ (21), which is then converted to hydrogen peroxide and other

reactive oxygen species (ROS). Unbalanced intracellular ROS level can lead to oxidative stress, causing DNA damage, lipid peroxidation, and can ultimately trigger apoptosis. We therefore hypothesize that honokiol may inhibit lung SCC by affecting mitochondrial function. In the present study, we used NTCU-induced preclinical mouse lung SCC model to evaluate the preventive efficacy of honokiol, and the impact of honokiol on mitochondrial respiration and function.

Materials and Methods

Reagents and animals

N-nitroso-trischloroethylurea (NTCU) was purchased from Toronto Research Chemicals, Inc. (Toronto, Canada). Acetone was purchased from Sigma (St. Louis, MO). Honokiol was purchased from LKT laboratories (St. Paul, MN).

Lung SCC was induced in mice through NTCU administration as previously reported (18, 22, 23). All studies on animals were approved by the Medical College of Wisconsin Institutional Animal Care and Use Committee. Six-to-eight weeks old female NIH Swiss mice were obtained from Charles River Laboratories (Wilmington, MA). Animals were housed with wood chip bedding in environmentally controlled, clean-air rooms with a 12-hour light-dark cycle and 50% relative humidity. Drinking water and diet were supplied *ad libitum*. NIH Swiss mice were randomized into two groups with twenty five mice per group. All mice were treated topically with 0.03 M NTCU in 100-microliter drop, twice a week, with a 3.5-d interval for 28 weeks. Two weeks after the start of NTCU treatment, mice in the control group were given vehicle (corn oil with 0.05% DMSO) and mice in test group were administered honokiol (dissolved in DMSO first, then diluted in corn oil, final DMSO concentration 0.05%) by oral gavage at concentration of 10 mg/kg body weight once a day, five days per week, for the duration of the studies. Throughout the studies, the health condition of the mice was monitored daily and body weights were measured weekly. Twenty-eight weeks after the initial treatment of NTCU, mice were euthanized by CO_2 asphyxiation. Lungs were fixed in zinc formalin overnight and stored in 70% ethanol for histopathology evaluation. Unlike lung adenocarcinomas, SCC does not form visible solid nodules on the surface of the lung. Serial tissue sections (5-μm each) were made from formalin-fixed lungs, and one in every 20 sections (approximately 100 μm apart) was stained with hematoxylin and eosin (H&E) and examined histologically under a light microscope to assess severity of tumor development (invasive SCC, SCC *in situ*, bronchial metaplasia, and bronchial hyperplasia,) as we reported previously (17).

Histopathology Analysis

The lesions, including invasive SCC, SCC *in situ*, and the bronchial hyperplasia/metaplasia, were scored from the H&E-stained sections of each lung by following the guidelines as described below. When hyperplasia occurs, a single layer of bronchiolar epithelial cells becomes multiple layers. The cells maintain their normal morphology. When bronchiolar metaplasia occurs, the normal columnar epithelium is replaced by flattened squamous epithelium with increased keratin production. When SCC *in situ* occurs, atypical cells (such as irregular shape, increased nucleus/cytoplasm ratio) with visible mitosis and loss of

orderly differentiation replace the entire thickness of the epithelium, although the bronchiole basement membrane remains intact, with no tumor cell invasion into the surrounding stroma. When invasive SCC occurs, general features of SCC such as keratin pearls, multiple nuclei, increasing mitotic index can be seen, and the normal architecture of the lung is disrupted. The lung SCCs area/lung lobe area ratio was evaluated using NanoZoomer Digital Pathology Virtual Slide Viewer software (Hamamatsu Photonic Co.). H&E-stained slides were scanned with the NanoZoomer HT slide scanner (Hamamatsu Photonics France SARL) and virtual slides analyzed and quantified.

Cell lines

Human lung SCC cell lines H226 and H520 were purchased from American Type Culture Collection (ATCC) in 2011, where they are regularly authenticated. Both cell lines were maintained in RPMI-1640 medium (Gibco) supplemented with 10% fetal bovine serum (FBS), penicillin (100 U/mL), and streptomycin (100 μg/mL).

Cell proliferation assay

Cell proliferation was assessed using the 3-(4,5-dimethylthiazol-2-yl)-2,5-diphenyltetrazolium bromide (MTT) method, according to standard protocols. Briefly, cells were seeded onto 96-well tissue culture plates at 10,000 cells per well. Twenty-four hours after seeding, cells were exposed to various concentrations of honokiol for 48 hours, while that of the control group was replaced with fresh medium. MTT (0.5 mg/ml) was added after the exposure period. The formazan crystals that formed were dissolved in Dimethyl Sulfoxide (DMSO) after 4-hour incubation and the absorbance was measured at 490 nm by Infinite M200 Pro plate reader (Tecan, Durham, NC). All assays were performed in triplicate.

Cell cycle analysis

Propidium iodine (PI) staining (BD Biosciences, San Diego, CA) was performed to analyze the cell cycle distribution of cells treated with honokiol relative to media controls in accordance with manufacturer's instructions. Briefly, 1×10^6 cells were treated with 60 μM honokiol for 6 and 24 hours. After collecting and washing twice with cold PBS, cells were resuspended in PBS containing annexin PI and RNase A. Cell preparations were incubated at 37°C for 30 min in the dark, and then analyzed with FACScalibur (BD Biosciences, San Diego, CA).

Caspase3/7 apoptosis assay

Honokiol induced apoptosis was analyzed by measuring caspase-3 activation using the CellPlayer Apoptosis Caspase-3/7 kit (Essen Bioscience) by following manufacturer's instructions. Briefly, 10,000 cells per well were seeded into 96-well plates, and allowed to adhere and grow overnight, reaching a confluence of ~25–35% confluence at the start of the assay. 16–24 hours later, cells were exposed to various concentrations of honokiol, and the probe staining cells with active caspase 3 (DEVD-NucView 488 caspase-3 substrate, Essen BioScience Ltd, Welwyn Garden City, UK) was added to each well at a final concentration of 5 μM. When added to the tissue culture growth medium, this inert, non-fluorescent

substrate freely crosses the cell membrane. Cleavage of the peptide by caspase-3 in the cytosol results in nuclear translocation of DNA-binding dye, which emits bright green fluorescence on binding to DNA. The cells were analyzed in the live-cell imaging instrument IncuCyte (Essen BioScience Ltd); appearance of green fluorescent nuclei of apoptotic cells was monitored and imaged over time. The Incucyte was programmed to image each well at 2-hour intervals. Data analysis was conducted using Incucyte 2011A software.

Extracellular flux assay

The bioenergetic function of H226 and H520 cells in response to honokiol was determined using a Seahorse Bioscience XF96 Extracellular Flux Analyzer (Seahorse Bioscience). Cells were seeded in specialized V7 Seahorse tissue culture plates 24 hours before the analysis, and maintained at 37°C in 5% CO_2. One hour before the start of the analysis, cells were washed and changed to unbuffered assay medium adjusted to pH 7.4, final volume 675 μL (MEM-α for MCF-7, DMEM/F12 for MCF-10A). After establishing the baseline oxygen consumption rate (OCR) and extracellular acidification rate (ECAR), various concentrations of honokiol were administered through an automated pneumatic injection port of XF96. The changes in OCR and ECAR were monitored for 4 hours. The resulting effects on OCR and ECAR are shown as a percentage of the baseline measurement for each treatment.

To determine the mitochondrial and glycolytic function of H226 and H520 cells in response to honokiol, we used the bioenergetic function assay previously described with several modifications (24). After seeding and treatment as indicated, cells were washed with unbuffered media as described above. Five baseline OCR and ECAR measurements were then taken before injection of oligomycin (1 μg/mL) to inhibit ATP synthase, FCCP (1–3 μmol/L) to uncouple the mitochondria and yield maximal OCR, and antimycin A (10 μmol/L) to prevent mitochondrial oxygen consumption through inhibition of complex III. From these measurements, indices of mitochondrial function were determined as previously described (24).

Intracellular ATP measurements

For ATP assays, cells were seeded at 1×10^4 cells per well in 96-well plates in complete media for 24 hours, honokiol at various concentration was added from 0 to 180 minutes. Relative adenosine triphosphate (ATP) levels were determined using a luciferase-based assay per manufacturer's instructions (Promega).

Redox status in subcellular compartments using roGFP

Cells were transfected with pEGFR-mito-roGFP (reduction-oxidation sensitive green fluorescent protein) using Lipofectamine 2000. After 48 hours of incubation in culture medium, stable expressing cells were selected using G418 for two weeks. After selection, 10,000 cells were seeded in blackwalled, clear-bottom 96-well plates (Corning, Tewksbury, MA) for 24 hours, cells were washed twice with HEPES buffer followed by treatment in triplicate with various concentrations of honokiol in HEPES buffer. Fluorescence intensities were measured on an Infinite M200 Pro plate reader (Tecan, San Jose, CA) with excitation at 400 or 480 nm and emission at 515 nm. The 400:480 nm ratios were determined after subtraction of background fluorescence measured with non-transfected cells. To confirm

subcellular localization of roGFP, cells cultured on cover slides were also exposed to PBS containing honokiol and MitoSOX (Invitrogen) for 20 min, after 3 washes with warm PBS, cells were fixed in 4% paraformaldehyde in PBS for 15 min, washed again and then mounted with mounting medium containing DAPI, and visualized under fluorescent microscopy using a 40× objective.

Statistical analysis

Data are presented as mean ± SE or mean ± SD, specified in different Figure legend. The data was analyzed by 2-tailed Student t test. *, $P < 0.05$; **, $P < 0.01$; ***, $P < 0.001$.

Results

Honokiol inhibits lung tumorigenesis in an NTCU-induced lung SCC mouse model

Recently, a study of honokiol in a xenograft lung tumor model demonstrated significant growth inhibition (25). However, this study utilized immunocompromised animal model, which limits their ability to assess the use of honokiol in a chemopreventive setting. To better assess the potential for honokiol to be used as a chemopreventive agent, testing the efficacy of honokiol in a mouse strain with chemically induced precancerous lesions would be necessary. In this study we used a NTCU-induced lung SCC model, which has been used for years in our lab as a successful mouse lung SCC model, which is organ specific and captures well-defined pathologic development from normal to bronchial hyperplasia, metaplasia, SCC *in situ*, and finally, SCC as seen in human (17–19). During the study, honokiol did not cause significant body weight loss in mice (data not shown). As shown in Fig. 1A and 1B, NTCU treatment caused the full spectrum of lesions, with the distributions of lesions as the following: normal (20.5 ± 1.7%), hyperplasia (42.3 ± 3.7%), metaplasia (12.8 ± 2.8%), and SCC (24.4 ± 3.6%). Among these different bronchial histology, normal, hyperplasia and invasive SCC represent most commonly observed histology. Honokiol, given by oral gavage at 10 mg/kg body weight dosage significantly reduced the percentage of SCC bronchial to 11.0% ± 3.3% (Fig. 1A, right panel and Fig. 1B, compare to control group, p value = 0.011). At the same time, honokiol increased the percentage of normal bronchial architecture to 38.5% ± 3.3% (compare to control group, p value = 0.004). Lung SCC phenotype was also further confirmed by nuclear p63 staining (Fig. 1A), which strongly stained poorly differentiated squamous cell in control group, and was decreased in honokiol treated mouse lungs. These results suggest that honokiol effectively blocked the progression to invasive SCC and could be a potential chemopreventive agent for lung SCC.

Honokiol suppresses cell growth, cell cycle progression and induced apoptosis both *in vitro* and *in vivo*

To investigate how honokiol inhibits lung SCC growth, we first determined the effect of honokiol on cell growth *in vitro* by testing on two human lung SCC cell lines, H226 and H520. Cells were treated with increasing concentrations of honokiol for 48 hours, and cell viability was assessed by MTT assay. As shown in Fig. 2A, honokiol treatment resulted in a dose-dependent growth inhibition of both human lung SCC cell lines, with H520 cells exhibiting relatively increased sensitivity to honokiol treatment.

The impact of honokiol treatment on cell cycle distribution was also analyzed. As shown in Fig. 2B, 45% to 50% cells are typically in the G1 phase in the control groups from both cell lines tested. A 6 hours exposure of lung SCC cells to 60 μM honokiol caused a slight increase in the percentage of cells accumulated in G1 phase, while 24 hours exposure to honokiol caused a significant accumulation of cells in G1/S phase, with the percentage of cells in G1/S phase increasing to 68% in H226 cells; and to 76% in H520 cells.

We also sought to analyze the impact of honokiol on apoptosis in these lung SCC cell lines. Caspases are aspartate-specific cysteine proteases that play a key role in mediating apoptosis. Caspases are sequentially activated due to cleavage of their inactive pro-caspase forms. The activation of caspase-3 results in the irreversible commitment of a cell to apoptosis. Therefore, the activation of caspase-3 is considered a reliable marker for cells undergoing apoptosis. To determine whether the reduction in cell viability was caused by apoptosis, we evaluated apoptosis induction of honokiol by caspase activity. As shown in Fig. 2C, cells treated with honokiol showed a significant increase in caspase 3/7 activity, which occurred in dose- and time-dependent manners (Fig. 2C).

To validate that honokiol has the same function in our *in vivo* NUCU-induced lung SCC model, we examined the extent of proliferation and apoptosis in lung tissue from control group and honokiol treated group. Imunohistochemical assays with anti-Ki67 antibody for proliferative index and cleaved caspase-3 antibody for apoptotic index were done. Staining for Ki-67 was present in 35.8% of tumor cells in the control group and it decreased to 11.7% in honokiol treated group. There was a significant increase in the number of cleaved caspase-3–positive cells in the lungs receiving honokiol compared with control mice (Fig. 2D). These results indicate that treatment with honokiol has the same effect, which decreased proliferation and induced apoptotic.

Honokiol suppresses mitochondrial function both *in vitro* and *in vivo*

Mitochondria are pivotal in controlling cell life and death, especially in the process of induction of apoptosis. Honokiol-induced mitochondrial dysfunction was investigated by both respiration measurement and determination of cellular ATP level. The basal rate of mitochondrial respiration, i.e. the rate that is not coupled to ATP synthesis was monitored on a XF96 Seahorse plate reader, which is capable of measure bioenergentic pathways, glycolysis and mitochondrial respiration. After established the baseline oxygen consumption rate (OCR), which reflects the rate of electron transport in mitochondria, increasing concentrations of honokiol were injected directly into assay wells. Honokiol caused a fast and concentration-dependent decrease in basal oxygen consumption rate (OCR) in both cell lines (Fig. 3A). Inhibition of cell respiration was detectable at honokiol levels as low as 6.25 μM (Fig. 3A Upper panel). At concentration of 50 μM, honokiol decreased the OCR by 60% in H226 cells and increased the ECAR by 50% (Fig. 3A Lower panel). Notably, ECAR, the surrogate marker for glycolysis, was stimulated in H226 cells due to possible compensation for the loss of OCR, but not increased in H520 cells. Mouse lung FFPE tissue from both control and honokiol group were also examined with cytochrome c staining, which is a known mitochondria marker, and is an electron-transport protein that localized in mitochondria. Our results showed that cytochrome c release was increased in honokil treated

mouse lung SCC tissue (Fig. 3B), which in line with our previous finding that honokiol induced caspase-3 cleavage, suggesting that honokiol may function through mitochondria.

Effect of honokiol on cellular bioenergetics

To further determine if the decreased OCR was functional, cells were treated with various concentrations of honokiol for 4 hours, and after thorough wash-out, addition of mitochondrial complex inhibitors, oligomycin, carbonylcyanide p-(trifluoromethoxy) phenylhydrazone (FCCP), and antimycin A, were sequentially injected to allow for the determination of six mitochondrial function parameters in cells, including basal respiration, ATP production, maximum respiratory capacity and reserved respiratory capacity. As shown in Fig. 4A, honokiol treatment caused a persistent and durable inhibition of basal OCR, evident even after honokiol was washed out. The addition of oligomycin allows a determination of the amount of oxygen consumed that is linked to ATP synthesis. The OCR after addition of FCCP is an estimate of the potential maximal respiratory capacity, which was decreased in a dose-depend manner upon honokiol treatment. The potential reserve capacity for bioenergetic function in the cells is then the maximal rate minus the basal rate. It is believed that the maximal respiratory capacity serves as an index of the ability of cells to respond to stress, such as ROS/RNS (reactive nitrogen species). All of these mitochondria function parameters were impacted after honokiol treatment in a similar manner (Fig. 4A) in both cell lines, with reserve capacity as the parameter most sensitive to inhibit by honokiol, indicating the lack of capacity to respond to stress after honokiol treatment. To further verify the effect of honokiol on mitochondrial metabolism, we evaluated cellular ATP levels, and found a dramatic decrease in cellular ATP content, evident even after relatively short exposure to honokiol, culminating in complete ATP depletion at a treatment concentration of 50 μM (Fig. 4B).

Honokiol inhibits mitochondrial respiration and decreases ATP levels in H226 and H520 cells, which may elevate AMP and the intracellular AMP/ATP ratio, leading to activation of the AMPK (5′ AMP-activated protein kinase) energy sensor signaling. The AMPK activation inhibits energy-consuming biosynthetic pathways (fatty acid and cholesterol syntheses), and the net result is attenuated tumor growth. We therefore examined AMPK pathway, cells treated with honokiol (50 μM) for varying lengths of time (0–30 min) were lysed, and separated on SDS-PAGE (sodium dodecyl sulfate-polyacrylamide gel electrophoresis), after probed with antibodies, we found that while total AMPKα protein level remained unchanged upon honokiol treatment, phosphorylated AMPKα (Thr172) was upregulated, indicating the activation of AMPK pathway. Once activated, AMPK directly phosphorylates and inactivates a number of ATP-consuming metabolic enzymes including acetyl-coenzyme A carboxylase (ACC). Increased phosphorylation of ACC in both cell lines were also observed in response to honokiol treatment as compared with untreated cells, whereas total ACC protein levels remain unchanged (Fig. 4C).

Honokiol promotes ROS production in mitochondria

Mitochondria appear to be the main intracellular source of ROS and other subsequent oxidants, which may damage DNA or other molecules, leading to apoptosis. To determine whether honokiol induces ROS production, we quantified intracellular ROS levels with a

recently developed Redox-sensitive green fluorescent protein (roGFP) probe. This probe consists of GFP with mutations emits at 400nm when oxidized, and at 480nm when reduced (26–28). This behavior allows the probe to monitor ROS production in real-time in different subcellular organelles via monitor 400/480nm ratio. In our study, we utilized roGFP targeted to the mitochondrial matrix (Fig. 5A), the co-localization of the ROS production in mitochondria was also confirmed with MitoSOX, the fluorogenic dye specifically targeted to mitochondria in live cells. Exposure to honokiol rapidly increased mitochondrial roGFP oxidation over controls dose-dependently (Fig. 5B), indicating that honokiol was able to promote mitochondrial ROS generation in human lung SCC cells.

Discussion

Chemoprevention, defined as using natural or chemical agents to slow or prevent the progression of carcinogenesis, was introduced around 30 years ago, and this strategy has shown promise in cancer control. Past research has shown reduced incidence of cancer in both high-risk groups and in the general population upon chemopreventive treatment (29, 30). Lung cancer, as the leading cause of cancer death in both men and women, is potentially traceable target for chemoprevention. Over the course of the past several decades, several promising chemoprevention agents have been identified (31–33); however, almost all of these agents have been studied in models of lung adenoma or lung adenocarcinoma. Therefore, it is critical to identify more appropriate therapeutic intervention for lung SCC. The use of the lung tumor progression model is more clinically relevant because it more closely parallels potential clinical chemoprevention trials by exposing mice with established precancerous lesions. In the present study, we examined the chemopreventive efficacy of honokiol in an initiation model of squamous cell lung cancer (SCC), which uses the carcinogen N-nitroso-trischloroethylurea (NTCU) and reliably triggers the development of SCC within 24–26 weeks. honokiol decreased the percentage of bronchioles with lung SCC histology accompanied with an increased percentage of normal bronchial histology, suggesting an inhibition of progression of bronchial cell hyperplasia to SCC lesions, thus providing a rationale for its further development as a chemopreventive agent for lung squamous cell carcinoma.

Unbalanced proliferation and inhibition of apoptosis in cancerous cells is believed to be one major mechanism for cancer progression. Apoptosis induction is associated with the anticancer activity of many chemoprevention agents. Honokiol was reported to be able to induce apoptosis through the loss of the mitochondrial membrane potential ($\Delta\Psi m$) (34), and combination with other apoptosis inducers, such as radiation (15), cisplatin (16), or even with a novel pro-apoptotic gene PNAS-4 (35), greatly promoted apoptosis in tumor cells. In this study, we further confirmed by apoptosis effector cleaved caspase-3 staining that honokiol was able to induce apoptosis in lung SCCs as well, which in turn would minimize aberrant cell proliferation and tumor promotion process.

Mitochondria have been attractive targets for cancer prevention due to its essential roles in maintaining the biosynthetic and energetic capacities of cancer cells, and are the primary sites of apoptosis. There has been growing interest in the recent years in exploring new approaches to interfering with or modulating mitochondrial function (e.g., respiration) as a

means to kill cancer cells (20). By measuring the oxygen consumption in the intact cell in real-time, herein we show that honokiol directly targets mitochondria, rapidly and persistently inhibiting mitochondrial respiration, and disrupting mitochondrial function by decreasing ATP generation as well as reducing the reserved respiratory capacity. Decreased ATP levels in both NSCLC cell lines triggered by honokiol treatment also led to elevated intracellular AMP/ATP ratio, and activation of the AMPK energy sensor signaling, which as the result may inhibit energy-consuming biosynthetic pathways (fatty acid and cholesterol syntheses), and finally attenuate tumor growth. Similar with honokiol, another well-known PPARγ agonist pioglitazone, was also found to decrease mitochondrial respiratory chain via direct binding to mitochondrial submit unit I (36). This may explains why both agents could increase the uptake of glucose, as once mitochondrial respiration is decreased, glycolysis pathway will compensate. However, compare to pioglitazone, honokiol doesn't have its side effect of adipogenic, which makes honokiol an ideal preventive agent for lung cancer.

ROS is the byproduct generated during normal mitochondrial respiration, however, is significantly increased when the electron transport chain is inhibited, or ATP generation is halted in mitochondria. Honokiol has been shown to induce cellular ROS generation in human hepatocellular carcinoma cells (30) and human prostate cancer cells (37), however, the exact mechanism of honokiol-triggered generation of ROS is not well understood. In the current study, through the use of the newly developed ROS probe, roGFP, here we are able, for the first time, to show that treatment of cells with honokiol induces rapid ROS accumulation in mitochondria, therefore, suggesting that a mitochondrion could be the potential source of intracellular ROS generated by the treatment of cells with honokiol. The constitutive intracellular redox environment dictates a cell's response to an agent that alters this environment (38). Transformed cells in the promotion stage of tumorigenesis have an enhanced ROS production, which would ultimately succumb these cells to apoptosis due to an uncontrollable production of reactive oxygen species. In contrast, normal cells most likely acquire resistance to transformation via adaption; therefore, the same pro-oxidative agent may stimulate cytoprotection in normal cells (38).

In conclusion, we demonstrate here that honokiol inhibits lung SCC development *in vivo*, induces apoptosis in both established human lung SCC cell lines as well as in NTCU-induced mouse lung SCC model, indicating the potential to be used in lung SCC prevention. We provide evidence which suggests that honokiol-induced apoptosis occurs through a mitochondrial damage-dependent pathway. It is likely that the inhibited ETC (electron transport chain), and resultant increased ROS generation play an important role in the efficacy of honokiol on carcinogenesis. Further mechanistic study of the relationship between mitochondrial ROS generation and permeability transition pore (MPT) induced by honokiol is essential to provide supporting information.

Acknowledgments

This work was supported by R01CA139959.

References

1. Sporn MB, Suh N. Chemoprevention of cancer. Carcinogenesis. 2000; 21:525–30. [PubMed: 10688873]
2. Lippman SM, Lee JJ, Sabichi AL. Cancer chemoprevention: progress and promise. J Natl Cancer Inst. 1998; 90:1514–28. [PubMed: 9790544]
3. Kelloff GJ, Sigman CC, Greenwald P. Cancer chemoprevention: progress and promise. Eur J Cancer. 1999; 35:2031–8. [PubMed: 10711244]
4. Xu HL, Tang W, Du GH, Kokudo N. Targeting apoptosis pathways in cancer with magnolol and honokiol, bioactive constituents of the bark of Magnolia officinalis. Drug Discov Ther. 2011; 5:202–10. [PubMed: 22466367]
5. Chiang CK, Sheu ML, Hung KY, Wu KD, Liu SH. Honokiol, a small molecular weight natural product, alleviates experimental mesangial proliferative glomerulonephritis. Kidney Int. 2006; 70:682–9. [PubMed: 16807544]
6. Liou KT, Shen YC, Chen CF, Tsao CM, Tsai SK. The anti-inflammatory effect of honokiol on neutrophils: mechanisms in the inhibition of reactive oxygen species production. Eur J Pharmacol. 2003; 475:19–27. [PubMed: 12954355]
7. Cohen MH, Williams GA, Sridhara R, Chen G, McGuinn WD Jr, Morse D, et al. United States Food and Drug Administration Drug Approval summary: Gefitinib (ZD1839; Iressa) tablets. Clin Cancer Res. 2004; 10:1212–8. [PubMed: 14977817]
8. Liou KT, Lin SM, Huang SS, Chih CL, Tsai SK. Honokiol ameliorates cerebral infarction from ischemia-reperfusion injury in rats. Planta Med. 2003; 69:130–4. [PubMed: 12624817]
9. Tsai SK, Huang SS, Hong CY. Myocardial protective effect of honokiol: an active component in Magnolia officinalis. Planta Med. 1996; 62:503–6. [PubMed: 9000881]
10. Hoi CP, Ho YP, Baum L, Chow AH. Neuroprotective effect of honokiol and magnolol, compounds from Magnolia officinalis, on beta-amyloid-induced toxicity in PC12 cells. Phytother Res. 2010; 24:1538–42. [PubMed: 20878707]
11. Lin YR, Chen HH, Ko CH, Chan MH. Neuroprotective activity of honokiol and magnolol in cerebellar granule cell damage. Eur J Pharmacol. 2006; 537:64–9. [PubMed: 16631734]
12. Atanasov AG, Wang JN, Gu SP, Bu J, Kramer MP, Baumgartner L, et al. Honokiol: a non-adipogenic PPARgamma agonist from nature. Biochim Biophys Acta. 2013; 1830:4813–9. [PubMed: 23811337]
13. Wang X, Duan X, Yang G, Zhang X, Deng L, Zheng H, et al. Honokiol crosses BBB and BCSFB, and inhibits brain tumor growth in rat 9L intracerebral gliosarcoma model and human U251 xenograft glioma model. PLoS One. 2011; 6:e18490. [PubMed: 21559510]
14. Wolf I, O'Kelly J, Wakimoto N, Nguyen A, Amblard F, Karlan BY, et al. Honokiol, a natural biphenyl, inhibits in vitro and in vivo growth of breast cancer through induction of apoptosis and cell cycle arrest. Int J Oncol. 2007; 30:1529–37. [PubMed: 17487375]
15. Zhou B, Yang L, Sun Q, Cong R, Gu H, Tang N, et al. Cigarette smoking and the risk of endometrial cancer: a meta-analysis. Am J Med. 2008; 121:501–8 e3. [PubMed: 18501231]
16. Jiang QQ, Fan LY, Yang GL, Guo WH, Hou WL, Chen LJ, et al. Improved therapeutic effectiveness by combining liposomal honokiol with cisplatin in lung cancer model. BMC Cancer. 2008; 8:242. [PubMed: 18706101]
17. Wang Y, Zhang Z, Yan Y, Lemon WJ, LaRegina M, Morrison C, et al. A chemically induced model for squamous cell carcinoma of the lung in mice: histopathology and strain susceptibility. Cancer Res. 2004; 64:1647–54. [PubMed: 14996723]
18. Wang Y, Zhang Z, Garbow JR, Rowland DJ, Lubet RA, Sit D, et al. Chemoprevention of lung squamous cell carcinoma in mice by a mixture of Chinese herbs. Cancer Prev Res (Phila). 2009; 2:634–40. [PubMed: 19584077]
19. Wang Y, Rouggly L, You M, Lubet R. Animal models of lung cancer characterization and use for chemoprevention research. Prog Mol Biol Transl Sci. 2012; 105:211–26. [PubMed: 22137433]
20. Pelicano H, Feng L, Zhou Y, Carew JS, Hileman EO, Plunkett W, et al. Inhibition of mitochondrial respiration: a novel strategy to enhance drug-induced apoptosis in human leukemia cells by a

reactive oxygen species-mediated mechanism. J Biol Chem. 2003; 278:37832–9. [PubMed: 12853461]

21. Saybasili H, Yuksel M, Haklar G, Yalcin AS. Effect of mitochondrial electron transport chain inhibitors on superoxide radical generation in rat hippocampal and striatal slices. Antioxid Redox Signal. 2001; 3:1099–104. [PubMed: 11813983]
22. Li JC, Zheng QJ, Jin CH, Ma RM. Circadian changes in the pharmacological effects of red ginseng saponins in mice. Zhongguo Yao Li Xue Bao. 1988; 9:22–6. [PubMed: 2461046]
23. Matsuda H, Namba K, Fukuda S, Tani T, Kubo M. Pharmacological study on Panax ginseng C. A. Meyer. III. Effects of red ginseng on experimental disseminated intravascular coagulation. (2). Effects of ginsenosides on blood coagulative and fibrinolytic systems. Chem Pharm Bull (Tokyo). 1986; 34:1153–7. [PubMed: 3731336]
24. Cheng G, Zielonka J, Dranka BP, McAllister D, Mackinnon AC Jr, Joseph J, et al. Mitochondria-targeted drugs synergize with 2-deoxyglucose to trigger breast cancer cell death. Cancer Res. 2012; 72:2634–44. [PubMed: 22431711]
25. Singh T, Prasad R, Katiyar SK. Inhibition of class I histone deacetylases in non-small cell lung cancer by honokiol leads to suppression of cancer cell growth and induction of cell death in vitro and in vivo. Epigenetics. 2013; 8:54–65. [PubMed: 23221619]
26. Hanson GT, Aggeler R, Oglesbee D, Cannon M, Capaldi RA, Tsien RY, et al. Investigating mitochondrial redox potential with redox-sensitive green fluorescent protein indicators. J Biol Chem. 2004; 279:13044–53. [PubMed: 14722062]
27. Meyer AJ, Dick TP. Fluorescent protein-based redox probes. Antioxid Redox Signal. 2010; 13:621–50. [PubMed: 20088706]
28. Klimova TA, Bell EL, Shroff EH, Weinberg FD, Snyder CM, Dimri GP, et al. Hyperoxia-induced premature senescence requires p53 and pRb, but not mitochondrial matrix ROS. FASEB J. 2009; 23:783–94. [PubMed: 18948382]
29. Hail N Jr. Mitochondria: A novel target for the chemoprevention of cancer. Apoptosis. 2005; 10:687–705. [PubMed: 16133861]
30. Hail N Jr, Lotan R. Cancer chemoprevention and mitochondria: targeting apoptosis in transformed cells via the disruption of mitochondrial bioenergetics/redox state. Mol Nutr Food Res. 2009; 53:49–67. [PubMed: 19051186]
31. Fu H, He J, Mei F, Zhang Q, Hara Y, Ryota S, et al. Lung cancer inhibitory effect of epigallocatechin-3-gallate is dependent on its presence in a complex mixture (polyphenon E). Cancer Prev Res (Phila). 2009; 2:531–7. [PubMed: 19470785]
32. Zhang Q, Fu H, Pan J, He J, Ryota S, Hara Y, et al. Effect of dietary Polyphenon E and EGCG on lung tumorigenesis in A/J Mice. Pharm Res. 2010; 27:1066–71. [PubMed: 20112129]
33. Ponnurangam S, Mammen JM, Ramalingam S, He Z, Zhang Y, Umar S, et al. Honokiol in combination with radiation targets notch signaling to inhibit colon cancer stem cells. Mol Cancer Ther. 2012; 11:963–72. [PubMed: 22319203]
34. Lai CS, Tsai ML, Cheng AC, Li S, Lo CY, Wang Y, et al. Chemoprevention of colonic tumorigenesis by dietary hydroxylated polymethoxyflavones in azoxymethane-treated mice. Mol Nutr Food Res. 2011; 55:278–90. [PubMed: 20718052]
35. Yuan Z, Liu H, Yan F, Wang Y, Gou L, Nie C, et al. Improved therapeutic efficacy against murine carcinoma by combining honokiol with gene therapy of PNAS-4, a novel pro-apoptotic gene. Cancer Sci. 2009; 100:1757–66. [PubMed: 19575751]
36. Garcia-Ruiz I, Solis-Munoz P, Fernandez-Moreira D, Munoz-Yague T, Solis-Herruzo JA. Pioglitazone leads to an inactivation and disassembly of complex I of the mitochondrial respiratory chain. BMC Biol. 2013; 11:88. [PubMed: 23915000]
37. Hahm ER, Singh SV. Honokiol causes G0-G1 phase cell cycle arrest in human prostate cancer cells in association with suppression of retinoblastoma protein level/phosphorylation and inhibition of E2F1 transcriptional activity. Mol Cancer Ther. 2007; 6:2686–95. [PubMed: 17938262]
38. Hail N Jr, Cortes M, Drake EN, Spallholz JE. Cancer chemoprevention: a radical perspective. Free Radic Biol Med. 2008; 45:97–110. [PubMed: 18454943]

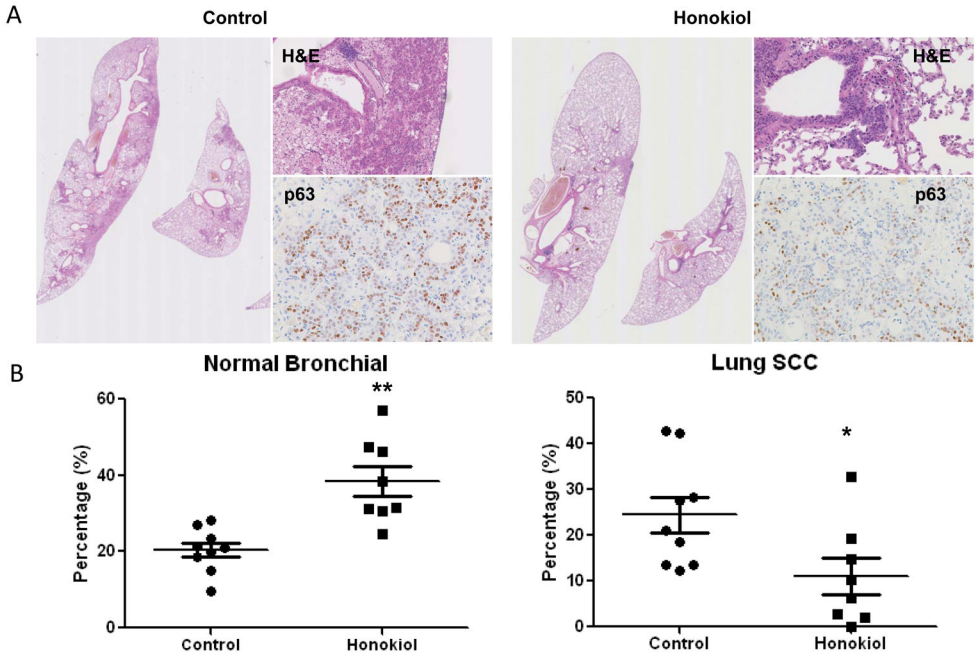

Figure 1.

Effect of honokiol on the development of lung SCCs. A, Typical H&E staining for mouse lung lubes from control group and honokiol treated group, upper panel, H&E showing the invasive SCC phenotype, lower panel, p63 staining. B, Effect of honokiol on lung SCC development based on the percentage of normal and SCC histopathology. As mouse SCC does not form visible solid nodules on the surface of the lung, serial tissue sections were made from each formalin-fixed lung and 1 in every 20 sections was stained with H&E. To assess specific effects of these agents on each histopathologic stage, all of the bronchi in each slide were counted and grouped into 5 categories based on normal, hyperplasia, metaplasia, SCC in situ (dysplasia was included in this category), and invasive SCC. The number in each category was then converted into percentage. Data shown are the means ± SE *, $P < 0.05$; **, $P < 0.01$.

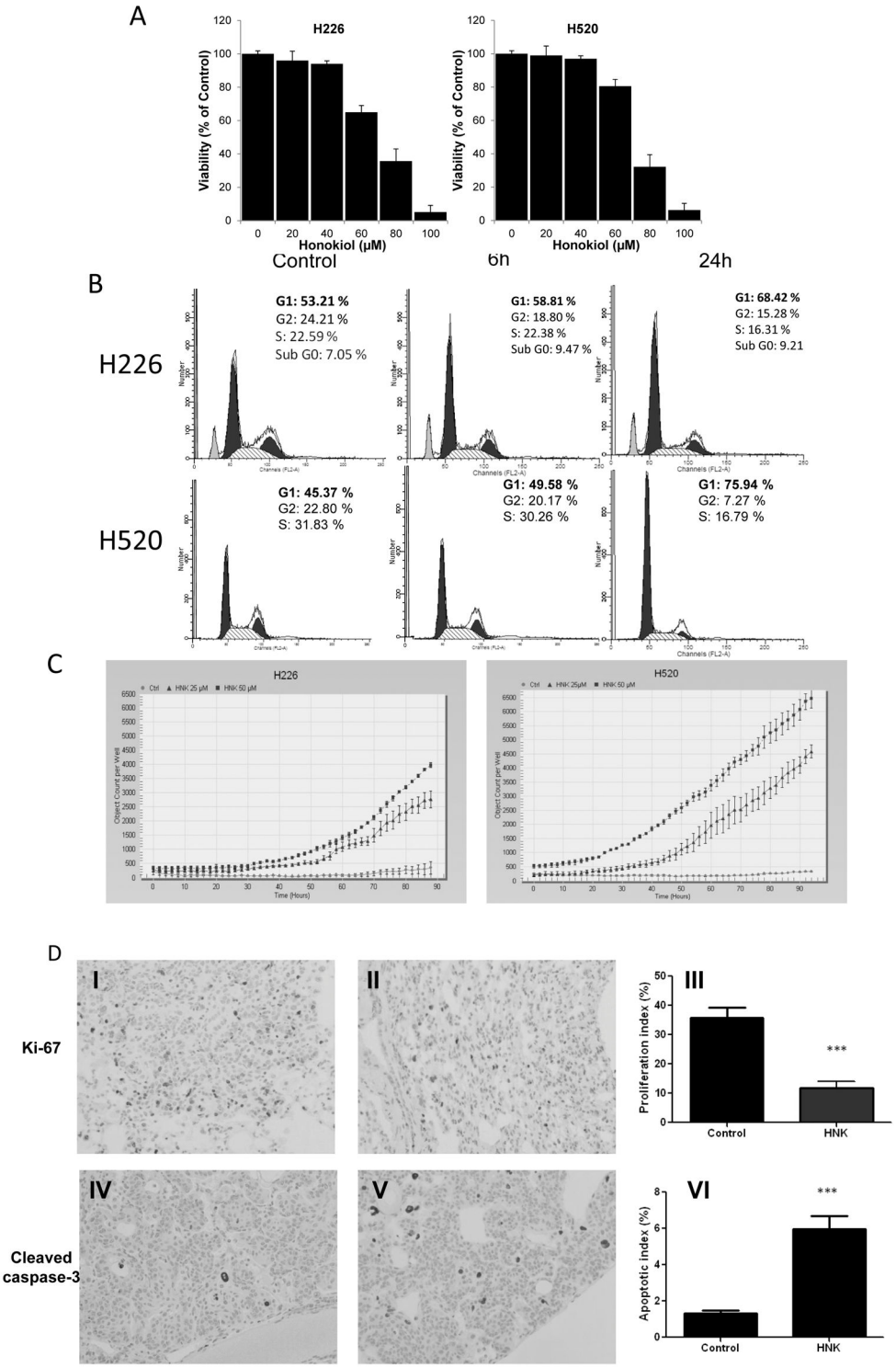

Figure 2.

Effect of honokiol on cell proliferation, cell cycle progression and apoptosis *in vitro* and *in vivo*. A, Relative cell proliferation rate of H226 and H520 cells treated with honokiol at various concentrations. B,. Effect of honokiol on cell cycle arrest. C, Effect of honokiol on

cleaved-caspase 3/7 staining. Shown is the caspase-3/7 fluorescence objects count from Incucyte. Data shown are the means ± SD (n = 3 per treatment group) D, Effect of honokiol on cell proliferation and apoptosis in NTCU-induced lung scc model. Lungs harvested from mice on the 26 weeks in NTCU study (n = 5 mice/group) were fixed, and the FFPE slides were stained using specific antibodies as detailed in the Materials and Methods section. I, II: Representative picture from immunohistochemistry for Ki-67 (I, control group; II, Honokiol group); III: proliferation index as determined by Ki-67; IV, V: Representative picture from immunohistochemistry for cleaved caspase-3 (III, control group; IV, Honokiol group). VI, apoptotic index as measured by cleaved caspase-3. ***, $P < 0.001$, control group versus honokiol group.

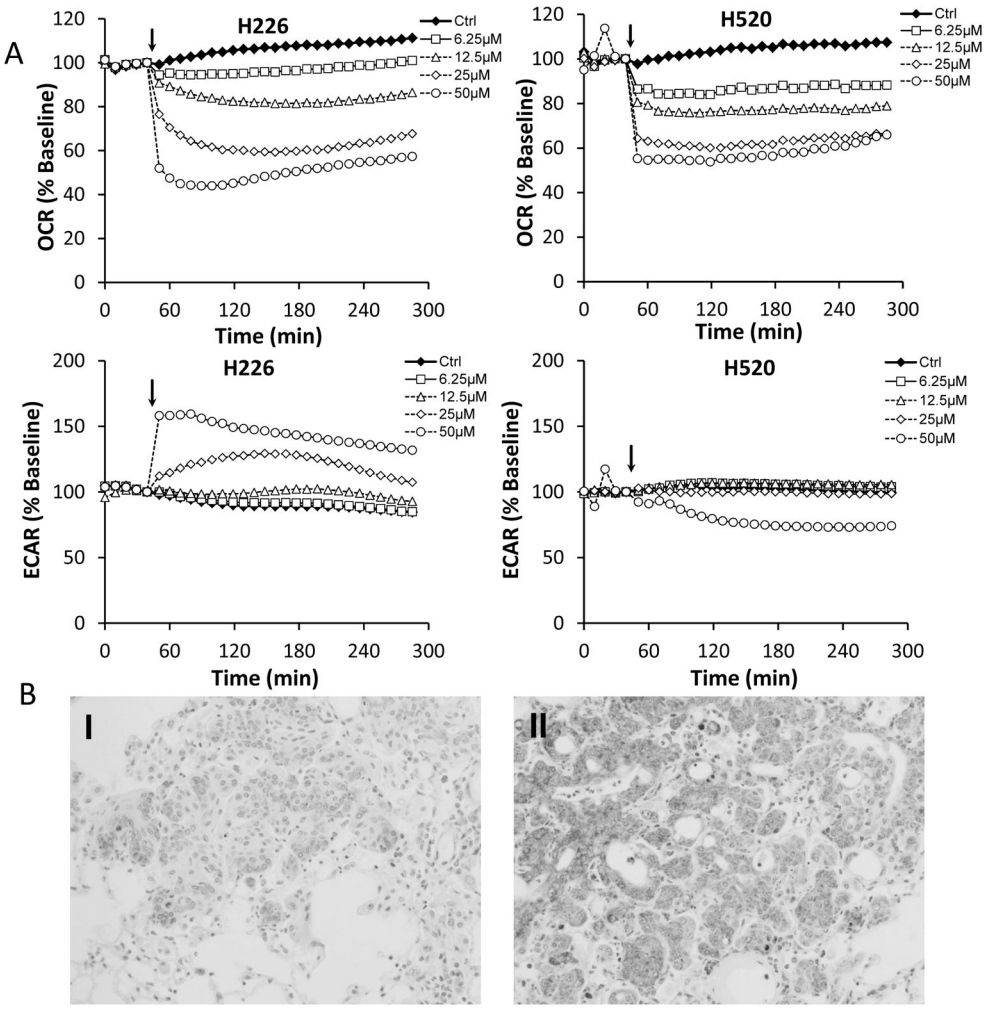

Figure 3. Honokiol suppresses mitochondria function both *in vitro* and *in vivo*

A, Bioenergetic profile of H226 and H520 cells treated with honokiol. H226 and H520 cells were seeded at 30,000 cells per well in specialized V7 Seahorse tissue culture plates. Changes in OCR (upper panel) and ECAR (middle panel) were monitored at 37°C for 4 hours. The resulting effects on OCR and ECAR are shown as a percentage of the baseline measurement for each treatment. Data shown are the means ± SE (n = 5 per treatment group). B, Effect of honokiol on mitochondria in NTCU-induced lung scc model. Lungs FFPE tissue slides (n = 5 mice/group) were stained using specific antibody against cytochrome C. I, II: Representative picture from immunohistochemistry for cytochrome c release (I, control group; II, Honokiol group).

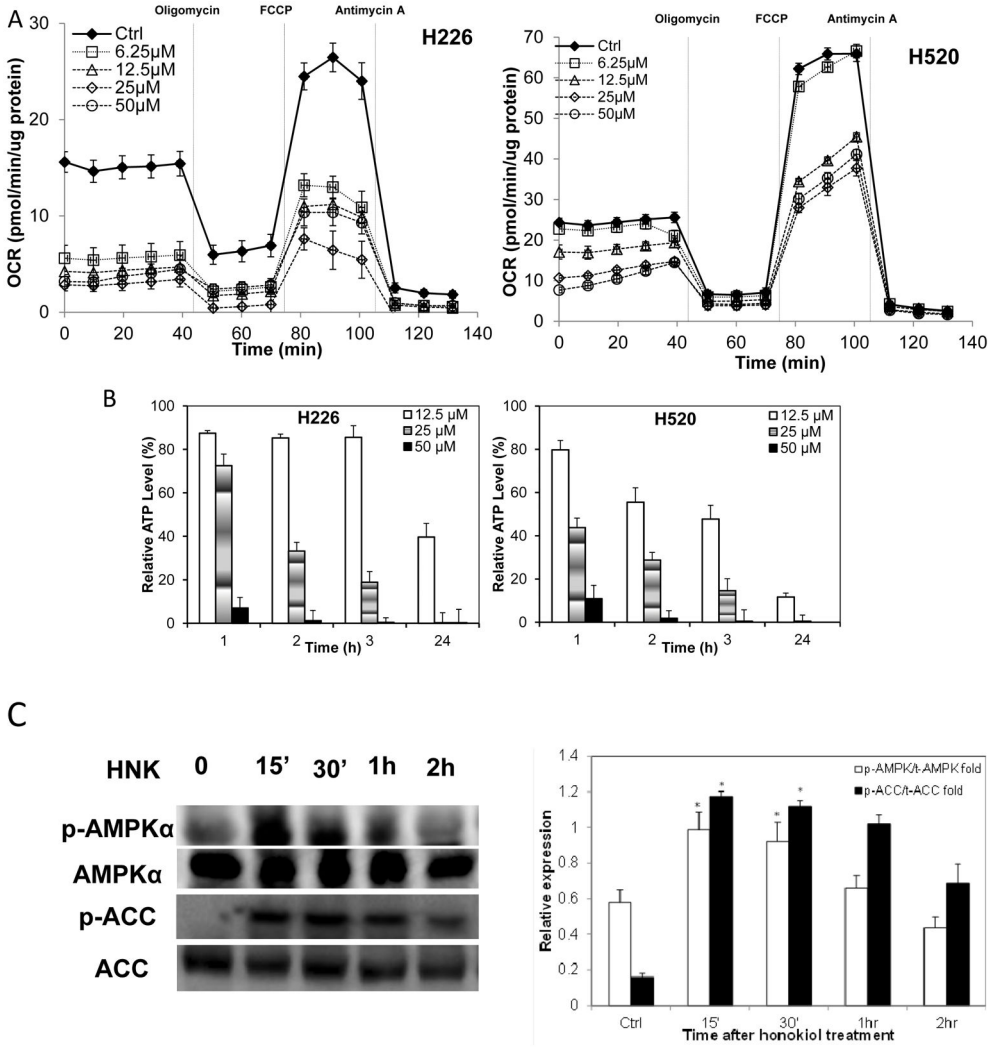

Figure 4.

The effects of honokiol on mitochondria function in H226 and H520 cells. A, Mitochondrial function upon honokiol treatment. Cells (20,000 cells per well) seeded in V7 culture plates were treated with honokiol at indicated concentrations for 4 hours, the cells were then washed with unbuffered media as described. Five baseline OCR and ECAR measurements were then taken before injection of oligomycin (1 μg/mL), to inhibit ATP synthase, FCCP (1–3 μmol/L) to uncouple the mitochondria and yield maximal OCR, and antimycin A (10 μmol/L) to inhibit complex III and mitochondrial oxygen consumption. The effects of honokiol on basal OCR, ATP-linked OCR and ECAR are shown. B, Honokiol caused ATP depletion in NSCLC cells. Cells were treated with honokiol for different time. Intracellular ATP levels were monitored using a luciferase-based assay. Data shown are the means ± SE, n=4 per treatment group. *, $P < 0.05$ versus control. C, Honokiol activated AMPK pathway. Left panel, western blotting analysis of AMPK pathway. Right Panel, optical band density analysis.

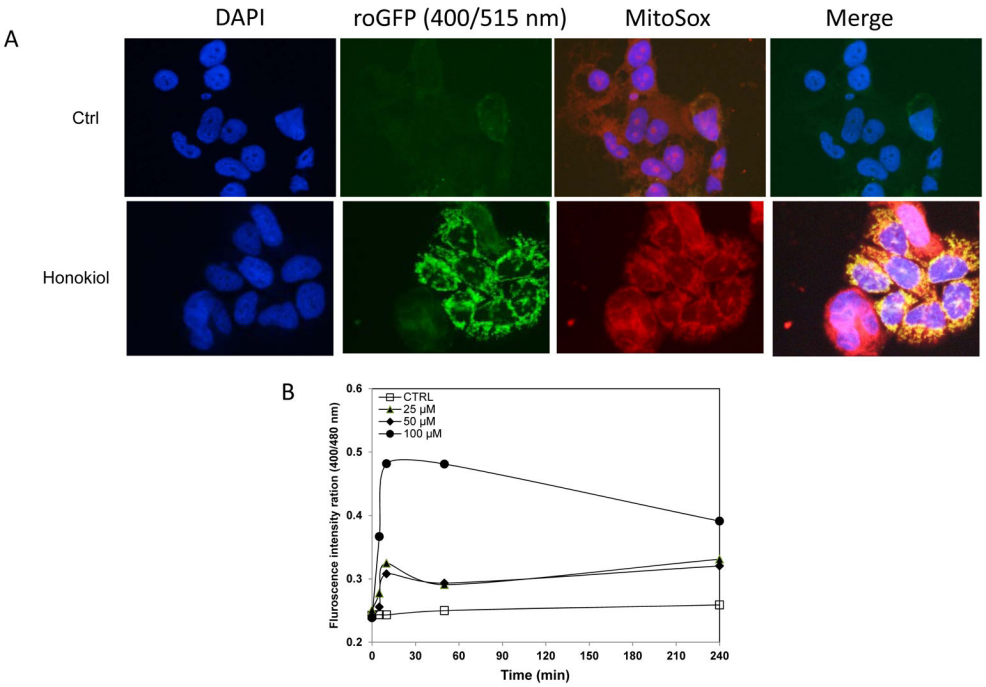

Figure 5.

Honokiol treatment shifts the mitochondria to a more oxidizing state. A, H520 cells with stable expression of pEGFP-mito-roGFP was stimulated with honokiol, Mito-EGFP-expressing H520 cells were loaded with MitoSOX Red (5 μM) for 20 min. roGFP states the production of ROS in mitochondria, which was also confirmed by MitoSOX red. Merged image shows co-localization of the mito-GFP fluorescence and MitoSOX Red (Mag. 40X). B, Honokiol promoted ROS production in NSCLC cells. Dual-excitation ratio measure (400/515nm and 480/515nm) with fluorescence plate reader was used to calculate ratiometric response from H520 cells after various concentrations of honokiol treatment at different time point.